Front. Environ. Sci. Eng. 2013, 7(3): 388–394
DOI 10.1007/s11783-012-0475-y

RESEARCH ARTICLE

# A Pt-Bi bimetallic nanoparticle catalyst for direct electro-oxidation of formic acid in fuel cells

**Shu-Hong LI[1], Yue ZHAO[1], Jian CHU[1], Wen-Wei LI[1], Han-Qing YU (✉)[1], Gang LIU[2], Yang-Chao TIAN[2]**

1 Department of Chemistry, University of Science and Technology of China, Hefei 230026, China
2 National Synchrotron Radiation Laboratory, University of Science and Technology of China, Hefei 230026, China



**Abstract** Direct formic acid fuel cells are a promising portable power-generating device, and the development of efficient anodic catalysts is essential for such a fuel cell. In this work Pt-Bi nanoparticles supported on micro-fabricated gold wire array substrate were synthesized using an electrochemical deposition method for formic acid oxidation in fuel cells. The surface morphology and element components of the Pt-Bi/Au nanoparticles were characterized, and the catalytic activities of the three Pt-Bi/Au nanoparticle electrodes with different Pt/Bi ratios for formic acid oxidation were evaluated. It was found that $Pt_4Bi_{96}$/Au had a much higher catalytic activity than $Pt_{11}Bi_{89}$/Au and $Pt_{13}Bi_{87}$/Au, and $Pt_4Bi_{96}$/Au exhibited a current density of 2.7 $mA \cdot cm^{-2}$, which was 27-times greater than that of Pt/Au. The electro-catalytic activity of the Pt-Bi/Au electrode for formic acid oxidation increased with the increasing Bi content, suggesting that it would be possible to achieve an efficient formic acid oxidation on the low Pt-loading. Therefore, the Pt-Bi/Au electrode offers a promising catalyst with a high activity for direct oxidation of formic acid in fuel cells.

**Keywords** catalyst, electrochemical deposition, formic acid oxidation, fuel cell, gold wire array, microfabrication

## 1 Introduction

Direct formic acid fuel cells (DFAFC) are a promising portable power-generating device due to their high electromotive force (a theoretical open circuit potential of 1.48 V), low fuel crossover flux through Nafion membrane and reasonable power density at low temperatures [1–6]. Recent studies on DFAFC have been focused on the development of efficient anodic catalysts [7–11] for the electro-oxidation of formic acid, which is one of the major hurdles for its commercialization.

A series of highly selective and active electrocatalysts have been reported to catalyze anodic oxidation in DFAFC. Among them, Pt and Pt-based bimetallic catalysts, such as Pt-Ru [12], Pt-Pd [13], Pt-Au [14] and Pt-Pb [15], have been extensively studied for the formic acid oxidation. Doping of a second metal not only enhances the catalytic activity, but also reduces the use of noble metal Pt and lower the cost [2,16]. Such an enhanced catalytic activity is attributed mainly to the decreased number of adsorption sites for CO as a result of "third-body effect", which increases the CO tolerance [17,18]. Recently, Bi, as a semimetal with unique properties of semimetal-semiconductor transition, has also been used to constitute Pt-Bi catalysts for formic acid oxidation [19,20].

Carbon materials have been widely used as supports for noble metal catalysts in fuel cells because of their attractive features of a high electrical conductivity, chemical stability and low cost [21–23]. Several other supporting substrates for catalyst, such as titanium [24], vanadium foil [25] and titanium nitride [26], have also been reported. The metal-supported catalysts generally have a high catalytic activity and stability for formic acid oxidation. Particularly, Au is recognized as an excellent substrate because of its good corrosion-resistance, high electrical conductivity and strong interaction with catalyst [27,28].

This work aimed to develop a novel Pt-Bi/Au catalyst for formic acid oxidation in fuel cells. In order to achieve such a goal, an easily-controllable method was developed to prepare a Pt-Bi/Au electrode. An integrated use of Ultraviolet (UV) lithography technology, argon ion-beam lithography and electrochemical deposition method was employed to prepare a gold wire array substrate to support Pt-Bi bimetallic nanoparticles (NPs) for formic acid oxidation. To explore the optimal components of the Pt-Bi/Au for formic acid oxidation, three Pt-Bi/Au catalysts

Received August 27, 2012; accepted November 7, 2012

E-mail: hqyu@ustc.edu.cn

with different Pt and Bi compositions were synthesized, and their formic acid oxidation performance was evaluated.

## 2 Experimental

### 2.1 Fabrication of the deposited gold wire array substrate

The fabrication of the gold wire array substrate was completed following a five-step process as described previously [29]. Prior to the fabrication, a glass substrate was washed with liquid detergent, rinsed with deionized water and acetone, and sequentially dried under ambient conditions. A thin layer of titanium and thick gold with a thickness of 500 nm were sputter deposited on the glass substrate. The thin layer of titanium was used as the adhesion between the glass substrate and the gold layer. Then, a positive photoresist (Suzhou Ruihong Co., China) with a thickness of 600 nm was spin-coated on the glass substrate. After soft-bake, the substrate was aligned and exposed using a photomask with the pattern of metal tracks. The exposed positive photoresist was then developed in 0.4% NaOH solution for 1 min. Later, ion-beam etching was conducted until the gold and titanium uncovered by the photoresist were completely removed. Subsequently, the remaining positive photoresist was removed using acetone. After cleaning, the gold wire array substrate as shown in Fig. 1 was fabricated. The gold film substrate was fabricated by sequentially sputtering titanium and gold on the glass substrate.

### 2.2 Preparation and characterization of Pt-Bi/Au nanoparticles

The Pt-Bi NPs were electrochemically deposited onto the gold wire array substrate using the cyclic voltammetry (CV) method. The electrochemical deposition solution contained 0.002 $mol \cdot L^{-1}$ $H_2PtCl_6$, three different concentrations (0.02, 0.01 and 0.004 $mol \cdot L^{-1}$) of $Bi(NO_3)_3$, and 40 $mL \cdot L^{-1}$ triethanolamine, dimethyl sulfoxide. The solution was deoxygenated with nitrogen gas prior to use. The scanning was conducted between $-0.8$ and $-1.1$ V (vs. Ag/AgCl) for 30 cycles at a scan rate of 50 $mV \cdot s^{-1}$. Then, the gold wire array substrate modified with the Pt-Bi NPs was rinsed respectively with acetone and deionized water, and was left to dry in air.

Pt-Bi/Au-film, Pt-Bi/indium tin oxide (ITO) and Pt/Au electrodes were also prepared using the electrochemical deposition method and used for the control experiment. Pt-Bi/Au-film and Pt-Bi/ITO were synthesized through depositing the Pt-Bi NPs onto the gold film and ITO substrate respectively. They were prepared using the same procedures for Pt-Bi/Au, except the electrochemical deposition solution, which contained 0.002 $mol \cdot L^{-1}$ $H_2PtCl_6$, 0.02 $mol \cdot L^{-1}$ $Bi(NO_3)_3$, and 40 $mL \cdot L^{-1}$ triethanolamine, dimethyl sulfoxide. Pt NPs were electrochemically deposited onto the gold wire array substrate with the CV method. Aqueous solution containing 0.5 $g \cdot L^{-1}$ $H_2PtCl_6$ and 0.1 $mol \cdot L^{-1}$ NaCl was used for the electrochemical deposition. The scanning was completed between $-0.5$ and 0.3 V (vs. Ag/AgCl) for 40 cycles at a scan rate of 50 $mV \cdot s^{-1}$.

The surface morphology of the Pt-Bi/Au catalysts was characterized using a scanning electron microscopy (SEM) (Sirion200, FEI Ltd., UK) at an accelerating voltage of 5–20 kV. The catalysts composition was analyzed with X-ray photoelectron spectrum (XPS, ESCALAB 250, Thermo-VG Scientific Co., USA).

### 2.3 Preparation of electrodes and electrochemical measurements

Electrochemical activities of the Pt-Bi/Au electrodes were

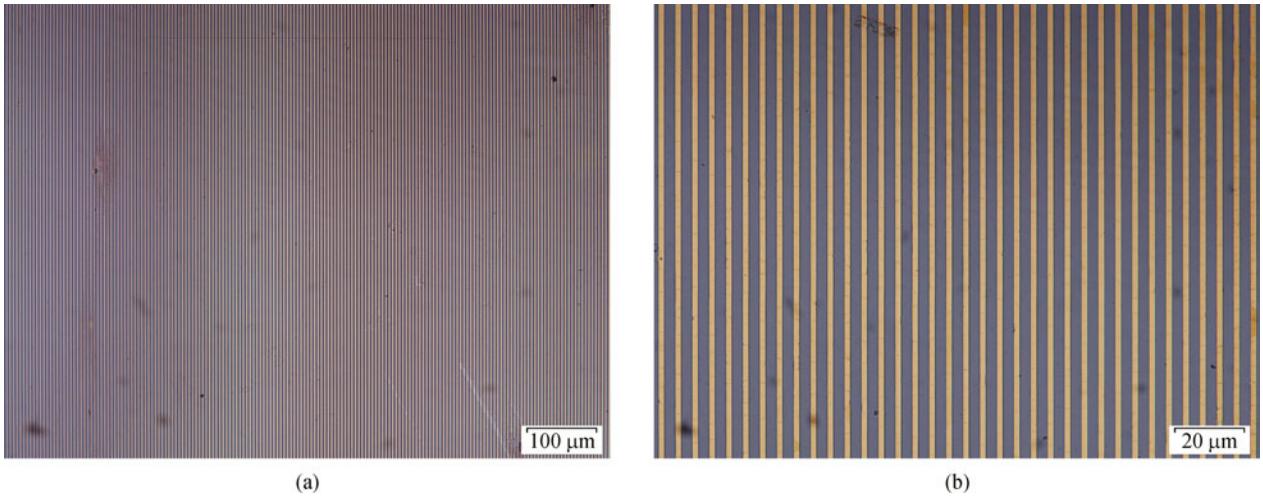


**Fig. 1** Images of the gold wire array substrate: (a) 10× optical zoom; and (b) 50× optical zoom

measured by CV and chronoamperometry on CHI842b electrochemical workstation (ChenHua Instruments Co., China) with a standard three-electrode system. Pt-Bi modified gold wire array substrate was used as the working electrode, while a platinum wire and an Ag/AgCl (saturated) electrode were respectively used as the counter and reference electrodes. The geometric surfaces areas of the electrodes were used to calculate the current density. A solution of 0.1 mol·L$^{-1}$ $H_2SO_4$/0.25 mol·L$^{-1}$ HCOOH was purged with nitrogen gas before the measurements. To evaluate the activities of the Pt-Bi/Au electrodes, CV analysis was performed in a potential between −0.2 and 1.0 V (vs. Ag/AgCl) at a scan rate of 10 mV·s$^{-1}$, whereas chronoamperometry was conducted in 0.1 mol·L$^{-1}$ $H_2SO_4$/0.25 mol·L$^{-1}$ HCOOH at 0.4 V (vs. Ag/AgCl) for 1 h.

## 3 Results and discussion

### 3.1 Gold wire array substrate

The comb-like gold wire array substrate (Fig. 1(a)) was fabricated using the UV exposure and argon ion-beam etching techniques. The gold wire had a width of 2 μm and the two adjacent gold wires had an interval of 3 μm (Fig. 1(b)). The unique structure of the gold wire array substrate made it conducive for the electrochemical deposition of the Pt-Bi NPs selectively at the edges on the gold wire surface, similar to the electrochemical step edge decoration [30,31].

### 3.2 CV for deposition of Pt-Bi NPs

Electrochemical deposition of Pt-Bi NPs onto the gold wire array substrate was performed in organic phase to prevent generation of bismuth oxide. Figure 2 shows the CV curve of the gold wire array substrate in the deposition solution. Two pairs of redox peak were observed and corresponded to $Bi^{3+}/Bi^0$ (I) and $PtCl_6^{2-}/Pt^0$ (II), respectively. The maximum reduction peak was found at −1.0 V.

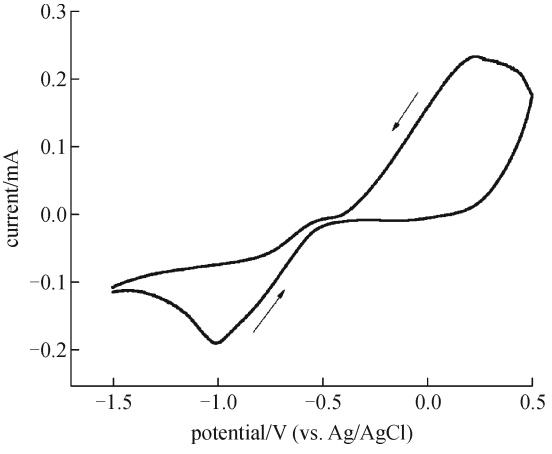


**Fig. 2** CVs of the gold wire array substrate in the electrochemical deposition solution (scan rate: 50 mV·s$^{-1}$, 0.002 mol·L$^{-1}$ $H_2PtCl_6$, 0.02 mol·L$^{-1}$ $Bi(NO_3)_3$, 40 mL·L$^{-1}$ triethanolamine, dimethyl sulfoxide)

### 3.3 XPS spectra

The XPS in Fig. 3(a) reveal the composition of the Pt-Bi NPs on the gold wire array substrate. The C 1s peak at 284.6 eV and O 1s peak at 532.8 eV were ascribed to the carbon and oxygen elements, respectively. The Bi $4f_{7/2}$ and Bi $4f_{5/2}$ peaks were observed at 159.7 eV and 163.2 eV, respectively. The peaks of Pt $4f_{7/2}$ and Pt $4f_{5/2}$, were at 71.2 and 74.2 eV, respectively. These results agree with those reported in literature well [20,32], confirming the presence of Bi and Pt elements. Table 1 lists the molar ratios of Pt and Bi in the three different catalysts, which were calculated from the peak areas of Pt and Bi (Fig. 3(b)).

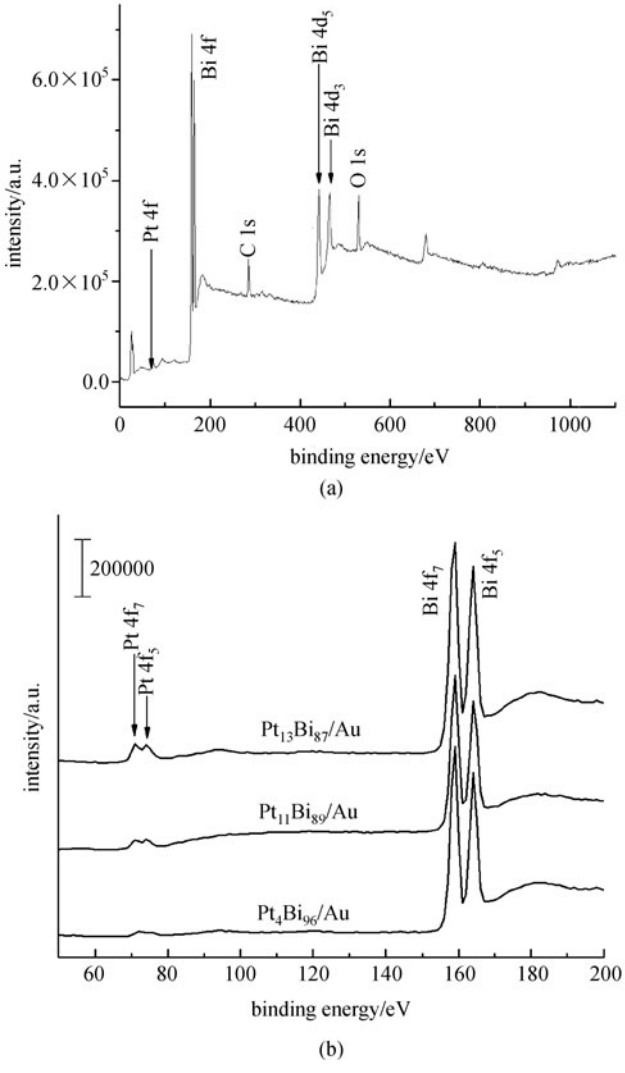


**Fig. 3** XPS of the Pt-Bi NPs supported on gold wire array substrate: (a) $Pt_4Bi_{96}$/Au; and (b) three different Pt-Bi/Au catalysts

**Table 1** Structural parameters of the Pt-Bi/Au catalysts

| catalyst | ratio of atomic wt.% of Pt and Bi | stoichiometry | molar ratio of Pt and Bi in deposition solutions |
|---|---|---|---|
| $Pt_4Bi_{96}$/Au | 3.98:96.02 | $PtBi_{24.1}$/Au | 1:10 |
| $Pt_{11}Bi_{89}$/Au | 10.61:89.39 | $PtBi_{8.43}$/Au | 1:5 |
| $Pt_{13}Bi_{87}$/Au | 12.71:87.29 | $PtBi_{6.87}$/Au | 1:2 |

The results clearly show that the three Pt-Bi/Au electrodes with different Pt/Bi atomic radios were synthesized using different electrochemical deposition solutions. The Bi content in the Pt-Bi NPs increased with the increasing $Bi(NO_3)_3$ content in the electrochemical deposition solution.

### 3.4 SEM characterization

Figure 4 shows the SEM images of $Pt_4Bi_{96}$/Au, $Pt_{11}Bi_{89}$/Au and $Pt_{13}Bi_{87}$/Au. The Pt-Bi NPs were found to distribute differently on the surface of the gold wire array substrate, depending on their compositions. The catalysts with a lower Pt content ($Pt_4Bi_{96}$/Au) showed non-homogeneous distribution of NPs with a particle diameter of 100 nm (Fig. 4(a)). This particle size was attributed to the agglomeration of the smaller particles (with a particle diameter of approximately 10 nm). The $Pt_{11}Bi_{89}$/Au and $Pt_{13}Bi_{87}$/Au catalysts exhibited larger particle diameters and the particles seemed to be cross-linked with each other and attached to the gold wire array substrate (Figs. 4(b) and (c)). Even although the same method was adopted for the synthesis, the Pt-Bi/Au NPs with different morphologies were obtained when different electrochemical deposition solutions were used. However, both the thickness of the gold wires and the size of the catalyst particles were large, attributed to the limitations of the UV exposure technology. Further efforts should be made to reduce the width of the gold wires. For example, with an integration of holographic lithography and microfabrication techniques, a gold nano-wire substrate with a width less than 100 nm could be prepared. Another possible option is the utilization of electron beam lithography, which can be used to pattern features of uniform size with a spatial resolution below 30 nm.

### 3.5 Electrochemical properties of Pt-Bi/Au electrode

To evaluate the electro-catalytic activity of the three Pt-Bi/Au catalysts, the CV of Pt-Bi/Au and Pt/Au electrocatalysts was conducted in 0.25 $mol \cdot L^{-1}$ HCOOH and 0.1 $mol \cdot L^{-1}$ $H_2SO_4$ as the supporting electrolyte. The peak currents in the forward scanning for $Pt_4Bi_{96}$/Au, $Pt_{11}Bi_{89}$/Au, $Pt_{13}Bi_{87}$/Au and Pt/Au, which was ascribed to the reaction of formic acid oxidation, were 2.7, 2.1, 0.87 and 0.10 mA $\cdot cm^{-2}$, respectively (Fig. 5). $Pt_4Bi_{96}$/Au exhibited a current density 1.3-fold greater than $Pt_{11}Bi_{89}$/Au, 3.1-fold greater than $Pt_{13}Bi_{87}$/Au and 27-fold greater than the Pt/Au. The current densities of the three Pt-Bi/Au electrocatalysts increased significantly, compared to the Pt/Au. Furthermore, the onset potential of $Pt_4Bi_{96}$/Au was lower than that of $Pt_{11}Bi_{89}$/Au or $Pt_{13}Bi_{87}$/Au. These results suggest that $Pt_4Bi_{96}$/Au had the highest activity for formic acid oxidation.

The current-decay pattern of the three Pt-Bi/Au and the

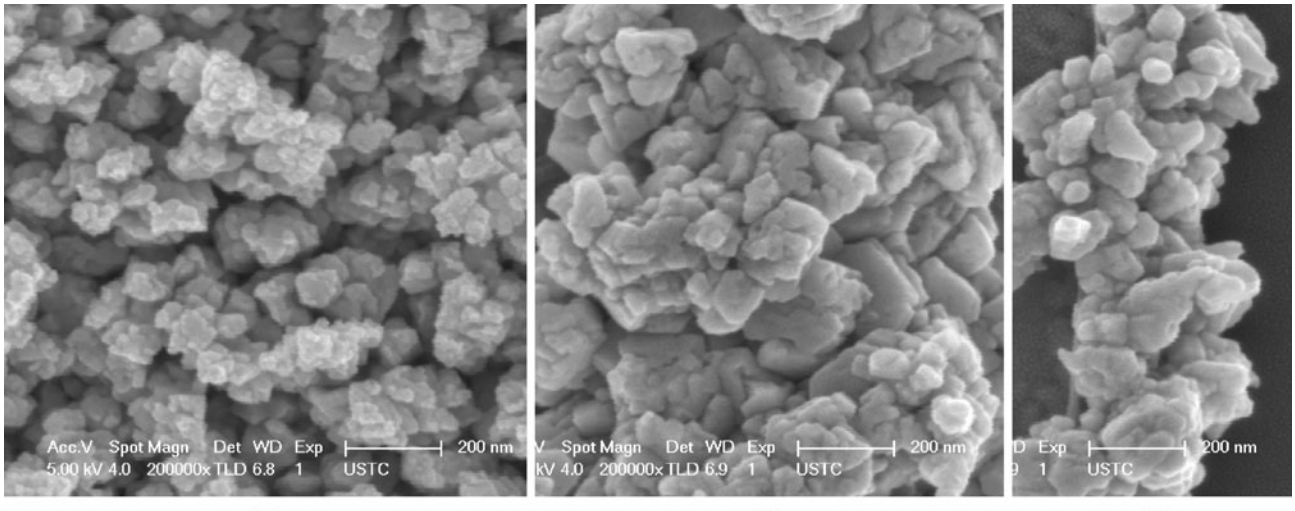


**Fig. 4** SEM images of the Pt-Bi NPs. (a) $Pt_4Bi_{96}$/Au; (b) $Pt_{11}Bi_{89}$/Au; and (c) $Pt_{13}Bi_{87}$/Au

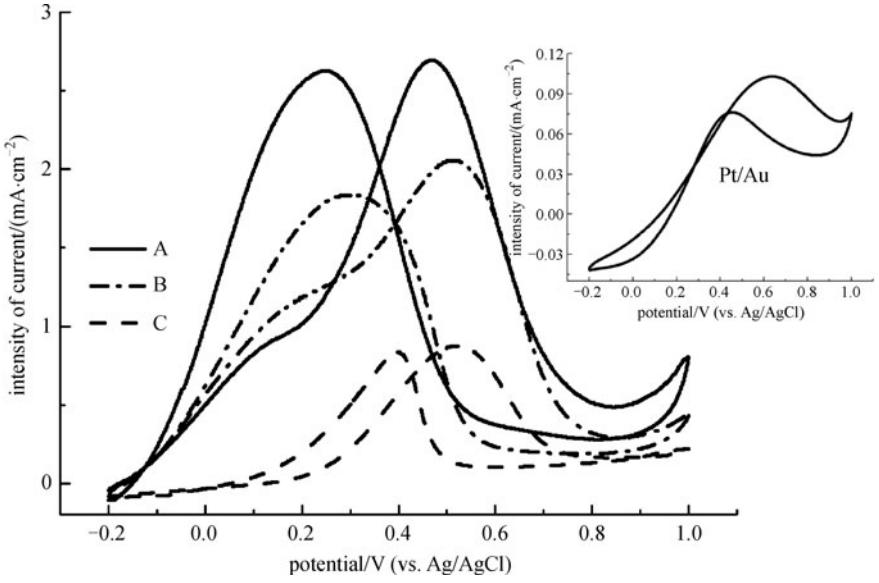


**Fig. 5** CVs of the three electrodes at a scan rate of 10 mV·s$^{-1}$ in 0.1 mol·L$^{-1}$ $H_2SO_4$, 0.25 mol·L$^{-1}$ HCOOH aqueous solution: (A) $Pt_4Bi_{96}$/Au; (B) $Pt_{11}Bi_{89}$/Au; and (C) $Pt_{13}Bi_{87}$/Au. The inset is the magnified CV of Pt/Au

Pt/Au catalysts at 0.4 V (vs. Ag/AgCl) in 0.1 mol·L$^{-1}$ $H_2SO_4$/0.25 mol·L$^{-1}$ HCOOH under ambient conditions is shown in Fig. 6. The current attenuation was rapid in the initial 15 min, and then slowed down. The final current values of the three electrodes after 1 h were in the following order: $Pt_4Bi_{96}$/Au > $Pt_{11}Bi_{89}$/Au > $Pt_{13}Bi_{87}$/Au > Pt/Au. This indicates that the current increased with the increasing Bi content in the catalysts. The higher catalytic activity of $Pt_4Bi_{96}$/Au than $Pt_{11}Bi_{89}$/Au and $Pt_{13}Bi_{87}$/Au was possibly attributed to the more regular morphology and smaller particle size, which is consistent with the above CV results.

In this study, photolithographic techniques and electrochemical deposition were used to fabricate the Pt-Bi/Au catalysts. As a result, the size and shape of Pt-Bi NPs were readily controlled by the gold arrays and could be modified easily. Compared with other methods, this approach provides much better control of the Pt-Bi NPs and has a high repeatability because of the micro-fabrication techniques used. With this approach, catalysts with a high catalytic activity could be prepared. Furthermore, the thickness of the gold wire array used in this work was only 500 nm, and such a thin layer of gold only costs about \$0.05 dollar·cm$^{-2}$. The extra costs are well worth the merits it brings about. Meanwhile, the Pt content of $Pt_4Bi_{96}$/Au catalyst with a higher catalytic activity was only 3.98% and the amount of noble Pt used could be reduced with this approach. Thus, the Pt-Bi/Au electrode prepared in this work offers a promising catalyst with a high activity for direct oxidation of formic acid in fuel cells.

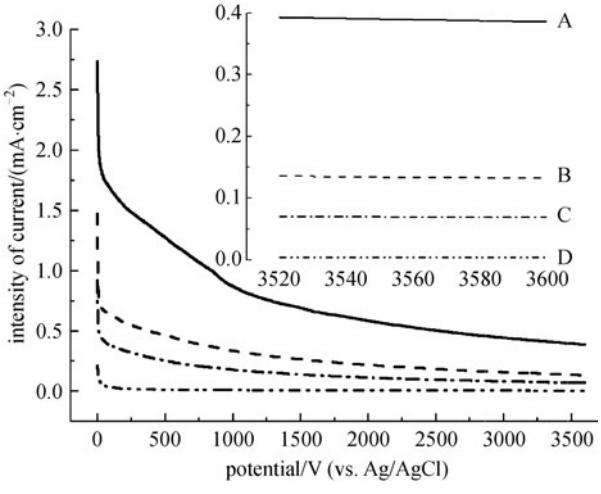


**Fig. 6** Chronoamperograms of the three electrodes at a scan rate of 0.4 V·s$^{-1}$ in 0.1 mol·L$^{-1}$ $H_2SO_4$, 0.25 mol·L$^{-1}$ HCOOH aqueous solution: (A) $Pt_4Bi_{96}$/Au; (B) $Pt_{11}Bi_{89}$/Au; (C) $Pt_{13}Bi_{87}$/Au; and (D) Pt/Au

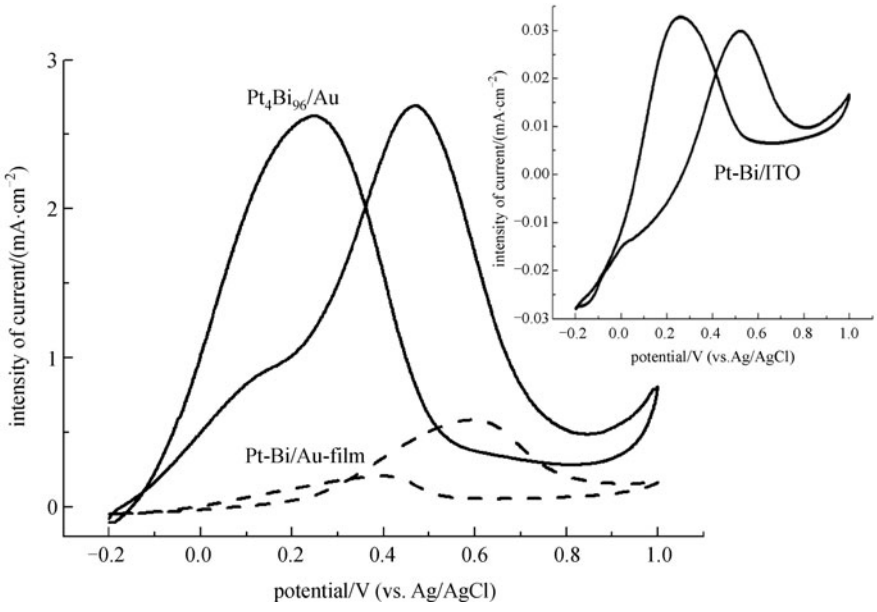


**Fig. 7** CVs of $Pt_4Bi_{96}$/Au, Pt-Bi/Au-film and Pt-Bi/ITO electrodes at a scan rate of 10 mV·s$^{-1}$ in 0.1 mol·L$^{-1}$ $H_2SO_4$, 0.25 mol·L$^{-1}$ HCOOH aqueous solution

### 3.6 Effect of the material substrate

To probe the effect of gold wire array on the Pt-Bi NPs activity, the Pt-Bi NPs were deposited onto the gold wire array, gold film and ITO, respectively, and the electro-catalytic activities of the three electrocatalysts were evaluated. Figure 7 illustrates the voltammetry at Pt-Bi/Au-film, Pt-Bi/ITO and $Pt_4Bi_{96}$/Au in 0.1 mol·L$^{-1}$ $H_2SO_4$/0.25 mol·L$^{-1}$ HCOOH solution. The current density from formic acid oxidation increased significantly for $Pt_4Bi_{96}$/Au and Pt-Bi/Au-film, compared to Pt-Bi/ITO. Meanwhile, $Pt_4Bi_{96}$/Au exhibited a current density almost 5-fold greater than Pt-Bi/Au-film. This might be attributed to the good corrosion-resistance, high electrical conductivity of Au substrate and strong interaction with Pt-Bi NPs. The results in Fig. 7 clearly show that the Au substrates had a much higher catalytic activity than the ITO, and the gold wire array was more suitable as a catalyst substrate. In addition, it was found that there was a synergistic effect between the Pt-Bi NPs and gold wire array. Future studies will be conducted to optimize the compositions of the Pt-Bi/Au and reduce the width of gold wires to further enhance its activity for formic acid oxidation in fuel cells.

## 4 Conclusions

An easily-controllable method was developed to prepare Pt-Bi/Au catalysts. Three Pt-Bi/Au catalysts with different compositions, i.e., $Pt_4Bi_{96}$/Au, $Pt_{11}Bi_{89}$/Au and $Pt_{13}Bi_{87}$/Au, were synthesized onto the gold wire array substrate and their performance for formic acid oxidation was evaluated. The electro-catalytic activity of Pt-Bi/Au for formic acid oxidation in acidic solution increased with the increasing Bi content, possibly attributed to the more regular morphology and smaller particle size.

**Acknowledgements** The authors wish to thank the National Natural Science Foundation of China (Grant No. 51129803), the National Synchrotron Radiation Laboratory (No. 20090160S) and the Fundamental Research Funds for the Central Universities (No. WK2060190007) for the support of this study.

## References

1. Wasmus S, Küver A. Methanol oxidation and direct methanol fuel cells: a selective review. Journal of Electroanalytical Chemistry, 1999, 461(1–2): 14–31
2. Antolini E. Palladium in fuel cell catalysis. Energy and Environmental Science, 2009, 2(9): 915–931
3. Youn D H, Bae G, Ham D J, Lee J S. Electrocatalysts for electrooxidation of methyl formate. Applied Catalysis A: General, 2011, 393(1–2): 309–316
4. Fang B Z, Kim M, Yu J S. Hollow core/mesoporous shell carbon as a highly efficient catalyst support in direct formic acid fuel cell. Applied Catalysis B: Environmental, 2008, 84(1–2): 100–105
5. Wang X, Hu J M, Hsing I M. Electrochemical investigation of formic acid electro-oxidation and its crossover through a Nafion® membrane. Journal of Electroanalytical Chemistry, 2004, 562(1): 73–80
6. Weber M, Wang J T, Wasmus S, Savinell R F. Formic acid oxidation in a polymer electrolyte fuel cell: a real-time mass-spectrometry study. Journal of the Electrochemical Society, 1996, 143(7): L158–L160
7. Liu Z L, Hong L, Tham M P, Lim T H, Jiang H X. Nanostructured Pt/C and Pd/C catalysts for direct formic acid fuel cells. Journal of

Power Sources, 2006, 161(2): 831–835
8. Xu C X, Liu Y Q, Wang J P, Geng H R, Qiu H J. Nanoporous PdCu alloy for formic acid electro-oxidation. Journal of Power Sources, 2012, 199(1): 124–131
9. Xu J B, Zhao T S, Liang Z X. Carbon supported platinum-gold alloy catalyst for direct formic acid fuel cells. Journal of Power Sources, 2008, 185(2): 857–861
10. Ha S, Larsen R, Zhu Y, Masel R I. Direct formic acid fuel cells with 600 $mA \cdot cm^{-2}$ at 0.4 V and 22°C. Fuel Cells (Weinheim), 2004, 4 (4): 337–343
11. Yu X W, Pickup P G. Codeposited PtSb/C catalysts for direct formic acid fuel cells. Journal of Power Sources, 2011, 196(19): 7951–7956
12. Waszczuk P, Barnard T M, Rice C, Masel R I, Wieckowski A. A nanoparticle catalyst with superior activity for electrooxidation of formic acid. Electrochemistry Communications, 2002, 4(7): 599–603
13. Rice C, Ha S, Masel R I, Wieckowski A. Catalysts for direct formic acid fuel cells. Journal of Power Sources, 2003, 115(2): 229–235
14. Choi J H, Jeong K J, Dong Y, Han J, Lim T H, Lee J S, Sung Y E. Electro-oxidation of methanol and formic acid on PtRu and PtAu for direct liquid fuel cells. Journal of Power Sources, 2006, 163(1): 71–75
15. Uhm S Y, Chung S T, Lee J Y. Activity of Pt anode catalyst modified by underpotential deposited Pb in a direct formic acid fuel cell. Electrochemistry Communications, 2007, 9(8): 2027–2031
16. Zhou X C, Xing W, Liu C P, Lu T H. Platinum-macrocycle co-catalyst for electro-oxidation of formic acid. Electrochemistry Communications, 2007, 9(7): 1469–1473
17. Herrero E, Fernández-Vega A, Feliu J M, Aldez A. Poison formation reaction from formic acid and methanol on Pt(111) electrodes modified by irreversibly adsorbed Bi and As. Journal of Electroanalytical Chemistry, 1993, 350(1–2): 73–88
18. Xia X, Iwasita T. Influence of underpotential deposited lead upon the oxidation of HCOOH in $HClO_4$ at platinum electrodes. Journal of the Electrochemical Society, 1993, 140(9): 2559–2565
19. Casado-Rivera E, Volpe D J, Alden L, Lind C, Downie C, Vázquez-Alvarez T, Angelo A C D, DiSalvo F J, Abruña H D. Electrocatalytic activity of ordered intermetallic phases for fuel cell applications. Journal of the American Chemical Society, 2004, 126(12): 4043–4049
20. Tripković A V, Popovic K D, Stevanovic R M, Socha R, Kowal A. Activity of a PtBi alloy in the electrochemical oxidation of formic acid. Electrochemistry Communications, 2006, 8(9): 1492–1498
21. Larsen R, Ha S, Zakzeski J, Masel R I. Unusally active palldaium-based catalysts for the electrooxidation of formic acid. Journal of Power Sources, 2006, 157(1): 78–84
22. Li X G, Hsing I M. Electrooxidation of formic acid on carbon supported $Pt_xPd_{1-x}$($x$ = 0–1) nanocatalysts. Electrochimica Acta, 2006, 51(17): 3477–3483
23. Liu H S, Song C J, Zhang L, Zhang J J, Wang H J, Wilkinson D P. A review of anode catalysts in the direct methanol fuel cell. Journal of Power Sources, 2006, 155(2): 95–110
24. Yi Q F, Chen A C, Huang W, Zhang J J, Liu X P, Xu G R, Zhou Z H. Titanium-supported nanoporous bimetallic Pt-Ir electrocatalysts for formic acid oxidation. Electrochemistry Communications, 2007, 9 (7): 1513–1518
25. Larsen R, Zakzeski J, Masel R I. Unexpected activity of palladium on Vandia catalysts for formic acid electro-oxidation. Electrochemical and Solid-State Letters, 2005, 8(6): A291–A293
26. Lee J M, Han S B, Song Y J, Kim J Y, Roh B, Hwang I, Choi W, Park K W. Methanol electrooxidation of Pt catalyst on titanium nitride nanostructured support. Applied Catalysis A: General, 2010, 375(1): 149–155
27. Umeda M, Ojima H, Mohamedi M, Uchida I. Methanol electro-oxidation at Pt-Ru-W sputter deposited on Au substrate. Journal of Power Sources, 2004, 136(1): 10–15
28. Jin C C, Sun X J, Dong R L, Chen Z D. Electrocatalytic oxidation of allyl alcohol on Pd and Pd-modified Au electrodes in alkaline solution. Applied Catalysis A: General, 2012, 431–432: 57–61
29. Chen Y P, Zhao Y, Qiu K Q, Chu J, Lu R, Sun M, Liu X W, Sheng G P, Yu H Q, Chen J, Li W J, Liu G, Tian Y C, Xiong Y. An innovative miniature microbial fuel cell fabricated using photolithography. Biosensors & Bioelectronics, 2011, 26(6): 2841–2846
30. Zach M P, Ng K H, Penner R M. Molybdenum nanowires by electrodeposition. Science, 2000, 290(5499): 2120–2123
31. Penner R M. Mesoscopic metal particles and wires by electrodeposition. Journal of Physical Chemistry B, 2002, 106(13): 3339–3353
32. Sanabria-Chinchilla J, Abe H, DiSalvo F J, Abruña H D. Surface characterization of ordered intermetallic PtBi(001) surfaces by ultra-high vacuum-electrochemistry. Surface Science, 2008, 602(10): 1830–1836